

Top-quark Pair plus Large Missing Energy at the LHC

Tao Han^{1,2}, Rakhi Mahubani^{2,3}, Devin G. E. Walker^{2,4}, Lian-Tao Wang^{2,5}

¹*Department of Physics, University of Wisconsin, Madison, WI 53706*

²*KITP, University of California, Santa Barbara, CA 93107*

³*Fermi National Acceleration Laboratory, Batavia, IL 60510*

⁴*Department of Physics, University of California, Berkeley, CA 94720 and Theoretical Physics Group, Lawrence Berkeley National Laboratory, Berkeley, CA 94720*

⁵*Department of Physics, Princeton University, Princeton, NJ. 08544*

ABSTRACT: We study methods of extracting new physics signals in final states with a top-quark pair plus large missing energy at the LHC. We consider two typical examples of such new physics: pair production of a fermionic top partner (a T' in Little Higgs models for example) and of a scalar top partner (a \tilde{t} in SUSY). With a commonly-adopted discrete symmetry under which non Standard Model particles are odd, the top partner is assumed to decay predominantly to a top quark plus a massive neutral stable particle A^0 . We focus on the case in which one of the top quarks decays leptonically and the other decays hadronically, $pp \rightarrow t\bar{t}A^0A^0X \rightarrow bj_1j_2\bar{b}\ell^-\bar{\nu}A^0A^0X + c.c.$, where the A^0 s escape detection. We identify a key parameter for the signal observation: the mass splitting between the top partner and the missing particle. We reconstruct a transverse mass for the lepton-missing transverse energy system to separate the real W background from the signal and propose a definition for the reconstructed top quark mass that allows it to take unphysical values as an indication of new physics. We perform a scan over the two masses to map out the discovery reach at the LHC in this channel. We also comment on the possibility of distinguishing between scalar and fermionic top partners using collider signatures.

Contents

1. Introduction	1
2. Signal Observability	3
2.1 Production Rates at the LHC	3
2.2 Extracting Top Partner Signal	5
2.3 Discovery Reach	12
3. Remarks on Distinguishing a Scalar Top Partner from a Fermion	14
4. Summary and Conclusions	17
5. Acknowledgement	18
A. Definitions of Transverse Variables	18
B. Top Reconstruction in Semileptonic Mode	19

1. Introduction

Although the Standard Model (SM) of elementary particle physics provides a very successful description of existing experiments at the highest energies currently accessible at colliders, it is anticipated that new physics will show up at the unexplored TeV-scale territory. High energy physics will thus experience the excitement of major discoveries in the next few years when the CERN Large Hadron Collider (LHC) opens up the new energy frontier. In addition to the long-awaited higgs boson, the particle responsible for the generation of mass, from naturalness arguments we hope to see a glimpse of some new physics at the LHC. Examples of popular scenarios of new physics include the Minimal Supersymmetric Standard Model (MSSM) [1] and its variants [2, 3]; models of new strong dynamics [4, 5, 6, 7, 8] or a composite Higgs at the TeV scale [9]; Little Higgs theories [10] and electroweak-scale extra dimensions [11, 12, 13]. Almost all these models contain a heavy particle which shares the gauge quantum numbers of the SM top quark, a ‘top partner’, which leads to a relatively generic class of collider signals from their production and subsequent decay. One of the main motivations for introducing such a particle is to cancel the quadratically divergent contribution to the Higgs mass from the SM top, which has a large yukawa coupling to the Higgs. This can come about using a scalar top partner, like the stop \tilde{t} in SUSY, or a fermionic one, like the T' heavy top in Little

Higgs models. We would expect these particles to show up naturally at an energy scale of order $4\pi v$, where $v \approx 246$ GeV is the Higgs field vacuum expectation value.¹

A necessary requirement for a viable new physics model is the suppression of the dimension-five and -six operators that are strongly constrained by the low energy data, such as electroweak precision measurements, CP violation or flavor changing neutral currents. In addition, dangerous baryon/lepton number violating operators must be forbidden or strongly suppressed. Motivated partly by these constraints and partly by being able to provide a possible candidate for Cold Dark Matter, many new physics scenarios incorporate a discrete symmetry under which the new physics particles carry the opposite charge to SM particles. Typical examples are R-parity in supersymmetry, KK-parity in UED, or T -parity in Little Higgs models [15, 16]. In such cases, assuming for minimality only a top partner (generically denoted by T , unless otherwise specified) and a stable neutral particle which is the lightest parity-odd state (A^0), the predominant decay mode of the top partner is

$$T \rightarrow tA^0. \quad (1.1)$$

leading to the following hadron collider signal:

$$pp \rightarrow T\bar{T} X \rightarrow tA^0 \bar{t}A^0 X \rightarrow t\bar{t} + \cancel{E}_T + X, \quad (1.2)$$

where X represents the beam remnant and other possible hadronic activity, and \cancel{E}_T is the missing transverse energy. It would be desirable to be able to distinguish between the different top partners that can give rise to this signal at the LHC.

The LHC will be a “top factory”: About 80 million SM $t\bar{t}$ events will be produced from pure QCD, in addition to another 34 million single-top events from the weak charged-current interaction for an integrated luminosity of 100 fb^{-1} . This provides a great opportunity to study properties of top quarks in detail. However, SM top quarks will also serve as a non-trivial background for any new physics signal with top quarks in the final state. Identifying such signals above the huge background has been the focus of several recent studies [17, 18, 19, 20]. In this article, motivated by the naturalness argument, we explore the signal of Eq. (1.2), concentrating on the semi-leptonic mode for the $t\bar{t}$ decays since the purely hadronic top decay mode has been studied previously [18, 20], with modest success. We optimize the kinematical cuts to separate the top partner signal from the SM backgrounds. In particular, we propose a reconstruction method for the top quark mass that allows it to take unphysical values to indicate the presence of physics beyond the SM. Furthermore, we comment on possible methods of determining the spin of the top partner. Such measurements would be crucial in distinguishing different underlying new physics scenarios, such as SUSY stop, or fermionic top partner pair production in UED or Little Higgs models with T -parity. We survey possible ways of getting relevant spin information for the new particle, and outline the difficulties involved.

¹Notice that exceptions to this argument are certainly possible. For example, in Twin Higgs models [14] the particle that cancels the quadratic divergence of the SM top loop does not have the quantum numbers of the top.

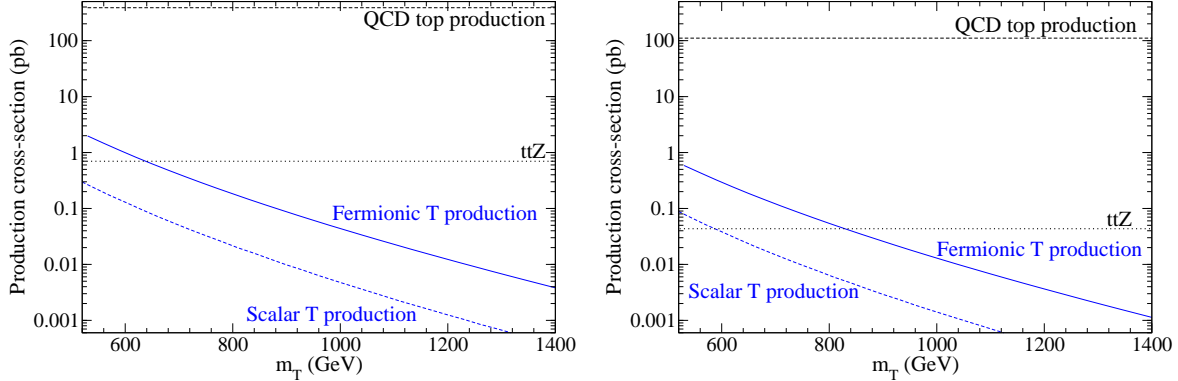


Figure 1: Leading order QCD cross section for top partner pair production at the LHC, as a function of its mass. The solid line corresponds to a spin- $\frac{1}{2}$ particle, the dashed line to a spin-0 state. The two dashed horizontal lines indicate the cross sections for the SM background processes $t\bar{t}$ and $t\bar{t}Z$ with tree-level matrix elements. The left panel shows the results before T decay, and the right panel includes the decay branching fractions to the semi-leptonic final state $bj_1j_2 \bar{b}\ell^{-}\bar{\nu} + \cancel{E}_T$, before any kinematical acceptance.

The rest of the paper is organized as follows. In Sec. II, we study the signal observability by carefully examining the kinematics and optimizing the background suppression. In Sec. III, we discuss the feasibility of spin and mass determination. We summarize and conclude in Sec. IV.

2. Signal Observability

In this section, we present a viable method for discovering new physics in the $t\bar{t} + \cancel{E}_T$ final state as in Eq. (1.2). We assume for the purpose of the following discussion that the top partner T is a color triplet under $SU(3)_C$ and a doublet under $SU(2)_L$.

2.1 Production Rates at the LHC

The leading production mechanism for the top partners is via QCD interactions

$$q\bar{q}, gg \rightarrow T\bar{T}. \quad (2.1)$$

In Fig. 1(a), we present the total leading order $T\bar{T}$ production cross section at the LHC as a function of the mass of the T . The solid line corresponds to a spin- $\frac{1}{2}$ particle; the dashed line corresponds to a spin-0 state. α_s is calculated at two loops, with the renormalization and factorization scales set equal to $\sqrt{s}/2$, and using the CTEQ 4M parton distribution functions [21]. We see from the figure a factor of 8 – 10 difference between the scalar and the fermion production cross sections. A factor of 4 comes from simple spin-state counting, and the remainder is due to threshold effects.

We will illustrate our procedure for background suppression using the example of a fermionic top partner only. Since we expect that the phase space will be the dominant factor in determining the kinematics, scalar top partner production and decay should have qualitatively the same behavior.

We assume that the fermionic top partner decays into a spin-1 neutral stable particle A^0 via a coupling:

$$(g_L \bar{t} \gamma^\mu P_L T + g_R \bar{t} \gamma^\mu P_R T) A_\mu^0 + h.c. \quad (2.2)$$

Generically, we expect this coupling to be chiral ($g_L \neq g_R$). In this study we choose $g_R = 0$ although we do not expect that alternative choices will significantly change our optimization method.

We focus on the semileptonic channel, with one top decaying hadronically and the other decaying leptonically

$$pp \rightarrow t\bar{t} A^0 A^0 X \rightarrow b j_1 j_2 \bar{b} \ell^- \bar{\nu} A^0 A^0 X + c.c. \quad (2.3)$$

where the charged leptons are $\ell = e, \mu$. The signal thus consists of an isolated charged lepton, two b -quark jets and two light-quark jets plus large missing energy. There are several advantages to studying this channel. First of all, the branching fraction of the semileptonic mode is sizable, about 6 times larger than the cleaner purely leptonic mode. Secondly, although the hadronic mode has a branching fraction that is 1.5 times larger still, the SM backgrounds for this mode are more severe than those for the semi-leptonic mode [18, 20]. Thirdly, one is able to distinguish the t from the \bar{t} using the charge of the lepton in the final state. The cross sections for this channel including decay branching fractions as a function of m_T are shown in Fig. 1(b).

Based on event topology we expect several SM processes to constitute the backgrounds to our signal. The leading SM background is QCD production of top quark pairs:

$$pp \rightarrow t\bar{t} X \rightarrow b j_1 j_2 \bar{b} \ell^- \bar{\nu} X + c.c. \quad (2.4)$$

The cross section for this process, depicted by the upper horizontal dashed lines in Fig. 1, is several orders of magnitude larger than our signal.

The next background with a large missing energy is

$$pp \rightarrow t\bar{t} Z X \rightarrow b j_1 j_2 \bar{b} \ell^- \bar{\nu} \nu \bar{\nu} X + c.c. \quad (2.5)$$

with $Z \rightarrow \nu \bar{\nu}$. As seen in Fig. 1 denoted by the lower horizontal dashed lines, even though the cross section for this process is smaller than the QCD $t\bar{t}$ by about a factor of 600, its kinematics are more similar to that of our signal, making such background events difficult to separate from the signal. We will elaborate on this below.

Another large SM background is from a process with no top quark

$$pp \rightarrow W b \bar{b} j_1 j_2 \rightarrow \ell^- \bar{\nu} b \bar{b} j_1 j_2 X + c.c. \quad (2.6)$$

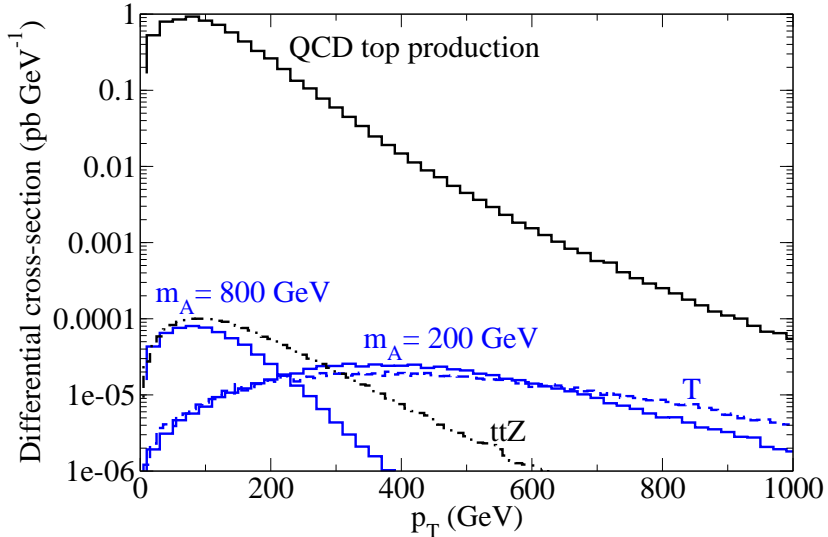


Figure 2: Transverse momentum distributions for the top quark from QCD $t\bar{t}$ production (the top curve), $t\bar{t}Z$ production (dot-dashed), and from T decays for $m_T = 1$ TeV and $m_A = 800, 200$ GeV, respectively. For comparison, we include the p_T of the fermionic T (long-dashed).

In our study, we simulate the SM $t\bar{t}$ and $t\bar{t}Z$ backgrounds using PYTHIA [22], while we use ALPGEN [23] for the $W(\rightarrow \ell\nu)bbjj$ background. We perform all calculations at parton level. With the stringent acceptance cuts to be discussed below, we expect that all next-to-leading order QCD effects, such as hadronization and initial and final state radiation, will not alter our results appreciably.

2.2 Extracting Top Partner Signal

In this section we present our main results on separating signal events from backgrounds. Although the SM backgrounds to the heavy top partner pair production and semileptonic decay are substantial, there are many kinematical differences between them that can be exploited. Moreover, we can take full advantage of the observation that the neutrino from W decay is largely responsible for the \cancel{E}_T in the $t\bar{t}$ and $Wbbjj$ backgrounds, while it contributes only a fraction of \cancel{E}_T in the signal.

A crucial parameter for the signal kinematics is the mass difference between T and A ,

$$\Delta M_{TA} \equiv m_T - m_A. \quad (2.7)$$

The energy of the top quark from T decay is $E_t \approx 0.5(1 + m_A/m_T)\Delta M_{TA}$ in the rest frame of the T . For a sufficiently large mass difference, the top quark can be very energetic. For a small ΔM_{TA} , however, the top quark has little kinetic energy and the signal kinematics

are very similar to those of the $t\bar{t}$ background. We will present results for two benchmark scenarios for illustration

$$m_T = 1 \text{ TeV}, \quad \text{and} \quad m_A = 200, 800 \text{ GeV}. \quad (2.8)$$

In Fig. 2, we show the transverse momentum distributions for the heavy T (dashed line), for the top quark from T decay for our two benchmark values, and from QCD $t\bar{t}$ (solid line), and $t\bar{t}Z$ (dot-dashed line). From this graph one can see that the p_T spectrum of the heavy T has the expected broad plateau near $(0.3 - 0.6)m_T$. The p_T spectrum of the top quark from T decay for small m_A is similar to that of the T quark itself, while for the small mass difference case ($m_A = 800 \text{ GeV}$), it is more similar to the $t\bar{t}$ background.

To simulate the detector acceptance [24, 25], we first impose the basic cuts

$$p_T^\ell > 20 \text{ GeV}, \quad |\eta_\ell| < 2.5, \quad \Delta R_\ell > 0.3, \quad (2.9)$$

$$E_T^j > 25 \text{ GeV}, \quad |\eta_j| < 2.5, \quad \cancel{E}_T > 25 \text{ GeV}, \quad (2.10)$$

$$E_T^b > 30 \text{ GeV}, \quad |\eta_b| < 2.5, \quad \Delta R_j, \Delta R_b > 0.4, \quad (2.11)$$

We adopt relatively small isolation cuts in order to accommodate the kinematics of a fast-moving top quark from a heavy T decay. We simulate the calorimetry responses for the energy measurements by adopting Gaussian smearing [24] with the following parameters:

$$\frac{\Delta E_e}{E_e} = \frac{10\%}{\sqrt{E_e(\text{GeV})}} \oplus 0.7\%, \quad \frac{\Delta E_j}{E_j} = \frac{50\%}{\sqrt{E_j(\text{GeV})}} \oplus 3\%. \quad (2.12)$$

We do not separately smear the muon momentum. In the energy-momentum range of current interest, the lepton resolutions should not make any appreciable difference in the results since the dominant effect is from hadronic smearing. We require two tagged b -jets in the selection. In our presentation of the discovery reach, we use a b -tagging efficiency of [24, 25]

$$\epsilon_b = 60\%, \quad (2.13)$$

which is appropriate for the range of p_T^b that we are interested in at low luminosity. In Fig. 3 we present some characteristic kinematical distributions for the signal and backgrounds with basic cuts imposed. The transverse mass variable M_T^{eff} is defined in Appendix A. The heavy T signal generically leads to energetic decay products unless the mass difference ΔM_{TA} becomes very small. From Fig. 3(b), we see that a large missing energy cut of $\cancel{E}_T > 350 \text{ GeV}$ could be imposed to effectively remove the $t\bar{t}Z$ backgrounds, but such a requirement will eliminate the signal in the case of small mass splitting $\Delta M_{TA} \sim 200 - 300$, where A^0 only carries away a small amount of kinetic energy $\sim 0.5(1 - m_A/m_T)(\Delta M_{TA} - m_t)$. As seen in Fig. 3(c), the effective transverse mass does not provide more discriminating power than \cancel{E}_T . There are in principle other transverse variables one could use to distinguish signal from background, such as the cluster transverse mass [26] (defined in Appendix A), or M_{T_2} [27]. However, these variables are largely similar, and unlikely to do significantly better than the \cancel{E}_T and M_T^{eff} variables presented here.

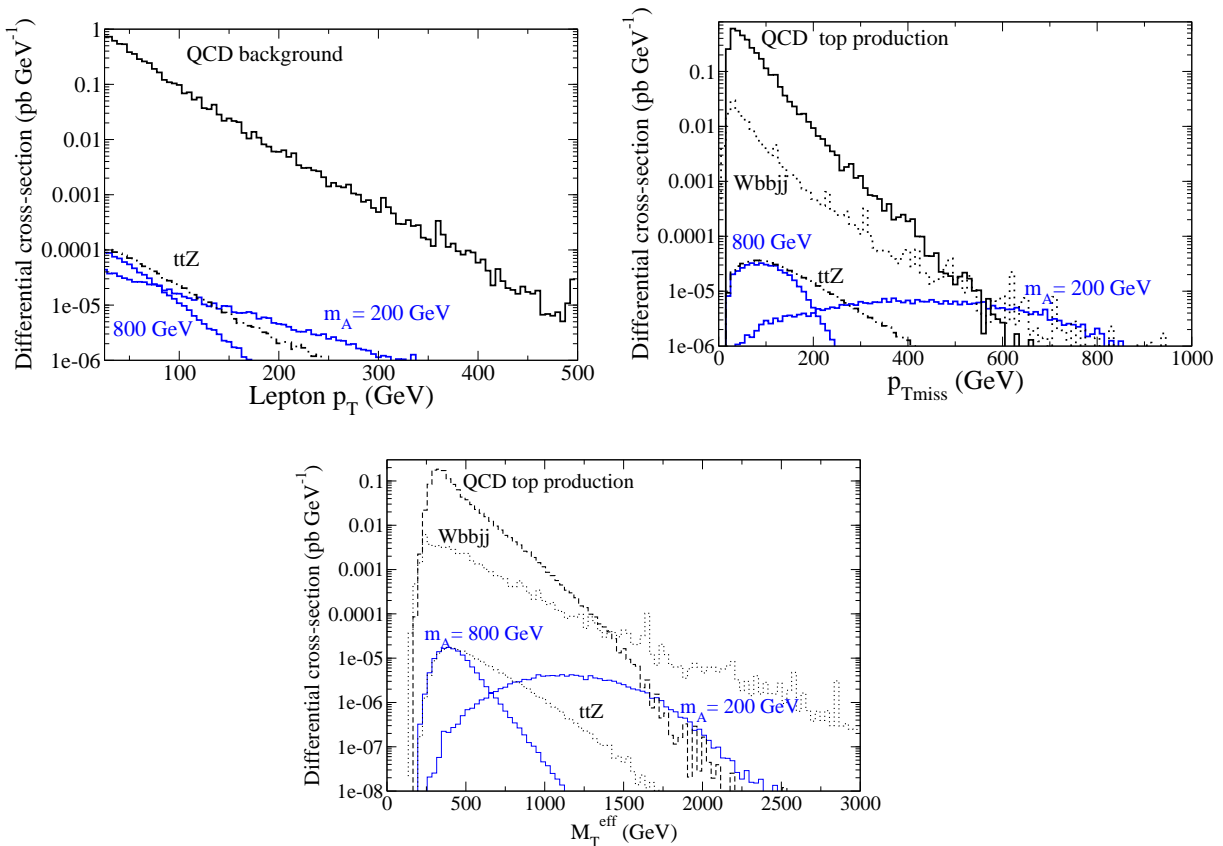


Figure 3: Differential distributions for (a) the transverse momentum of the charged lepton $p_T(\ell)$, (b) the missing transverse momentum $p_T^{miss} = \cancel{E}_T$, and (c) the effective transverse mass of the final state system, respectively.

As recently suggested in [20], one may consider exploring the correlation between \cancel{E}_T and M_T^{eff} , which we present in Fig. 4 for (a) the QCD $t\bar{t}$ background, (b) and (c) $T\bar{T}$ pair production with $\Delta M_{TA} = 200, 800$ GeV respectively. Two remarks are in order. First, the correlation is more distinctive between the signal and background when the mass difference ΔM_{TA} is large as seen in Fig. 4(b), namely $M_T^{\text{eff}} \sim 2\cancel{E}_T \sim 2m_T$. It tends to be very similar to the $t\bar{t}$ background distribution when $\Delta M_{TA} \sim m_t$ as in Fig. 4(c). This less desirable situation was not considered in [20] due to their parameter choice in favor of a dark matter candidate, in the context of a particular model [15]. Second, due to the overwhelmingly large rate of the $t\bar{t}$ background, this correlation variable alone is not sufficient to separate the signal in the semi-leptonic channel, as seen for the integrated rates by the color codes in Fig. 4.

There are other kinematical features that one could utilize to separate the signal from the backgrounds. One such variable is the transverse angle between the t and \bar{t} : We expect t pairs from pure QCD production to be co-planar in the $2 \rightarrow 2$ scattering plane and thus

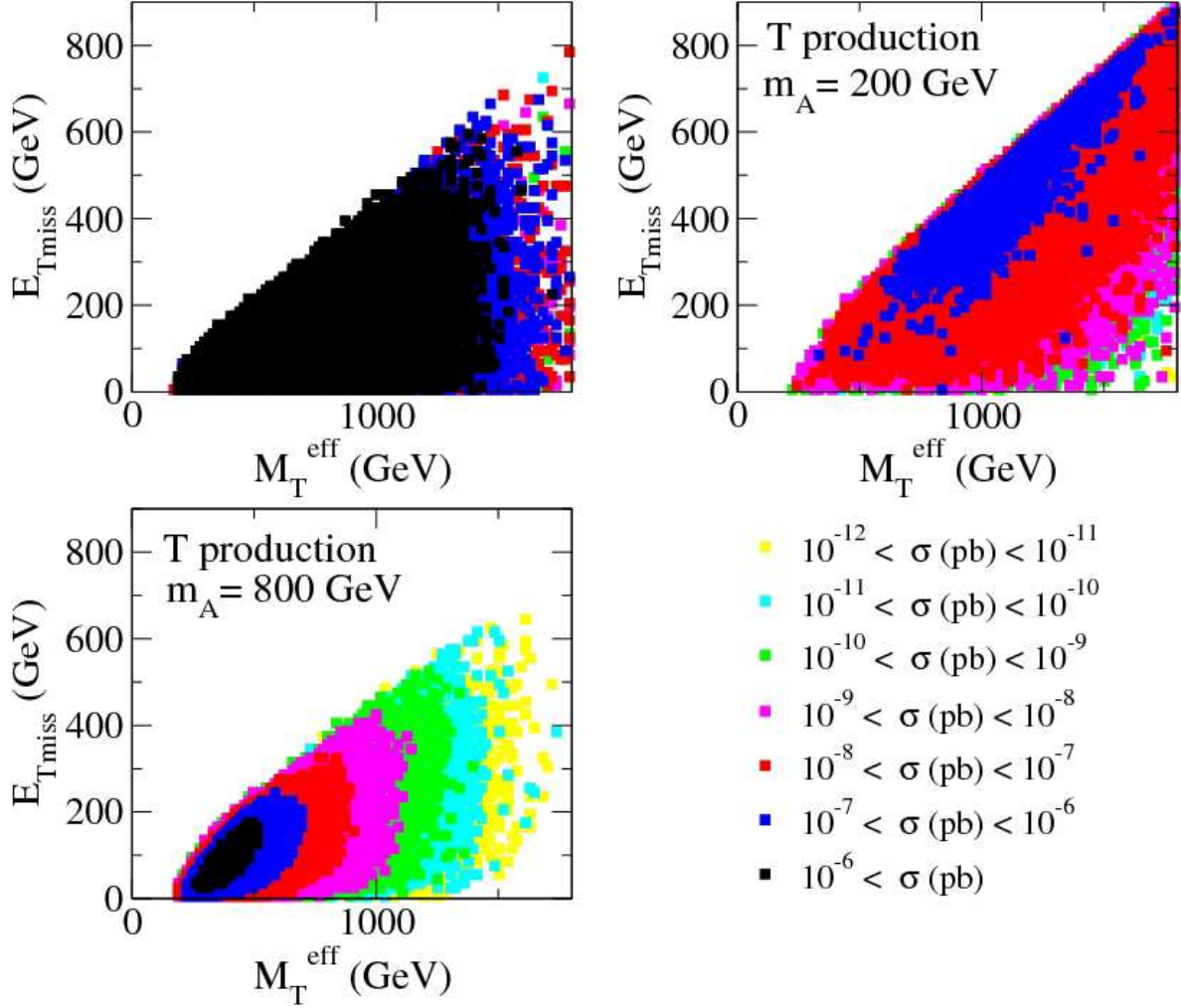


Figure 4: Kinematical correlation of events between E_T and M_T^{eff} for (a) the QCD $t\bar{t}$ background, (b) and (c) the T signal with $m_A = 200, 800$ GeV respectively. The color codes indicate the size of the cross sections.

back-to-back in the transverse plane, while those originating from $T\bar{T}$ decays will be more randomly oriented due to the transverse kicks of the missing A^0 particles. Although it is difficult to observe this co-planarity by studying the decay products of the top quarks due to the presence of the neutrino, one could still exploit the back-to-back nature of the $t\bar{t}$ background by evaluating the opening angle in the transverse plane between the hadronic top and the reconstructed momentum $\vec{p}_{bl} = \vec{p}_b + \vec{p}_l$, called ϕ_{t-bl} . For the $Wb\bar{b}jj$ background, we followed the same reconstruction procedure as the signal and other backgrounds (more details below) with ϕ_{t-bl} in this case defined by the angle between hadronic “top” and the unused \vec{p}_{bl} . We plot this distribution, rescaled by the total cross section, in Fig. 5. Indeed we see a strong correlation for $t\bar{t}$, $Wb\bar{b}jj$ and $t\bar{t}Z$, while the distribution for the signal is rather

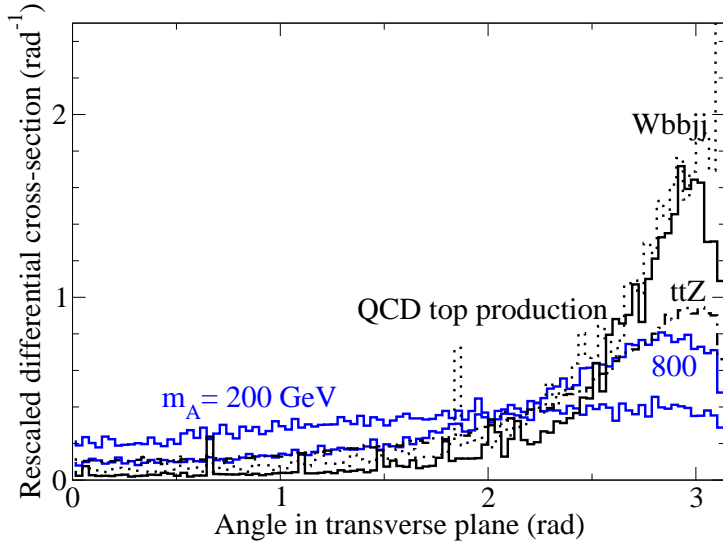


Figure 5: Normalized opening angle distributions in the transverse plane ϕ_{t-bl} for the signal $m_A = 200, 800$ GeV (solid), and the $t\bar{t}$ background (solid), $Wb\bar{b}jj$ (dashed), and $t\bar{t}Z$ (dot-dashed).

flat, especially when ΔM_{TA} is sizable. The discriminatory power of this variable decreases as the mass splitting becomes smaller. In addition this correlation will become less pronounced on inclusion of realistic QCD radiation and parton showering. We will therefore not devise a specific cut on this variable, although this could be implemented in a full optimization procedure.

Another obvious variable we might cut on is the di-jet mass, which will reconstruct a W for the signal, but not so for the background $Wb\bar{b}jj \rightarrow \ell\nu b\bar{b}jj$. This has been used in the top quark signal analysis at the Tevatron and we will take full advantage of this fact in our analysis.

Next, we turn to a discussion of reconstructing intermediate particle masses using kinematical variables. The first variable one might reconstruct is the transverse mass of the leptonically-decaying W by assuming $p_{\nu T} = E_{\nu T} = \not{p}_T$. As usual we define the transverse mass for the leptonic system as

$$M_T^2(W) = (E_{\ell T} + E_{\nu T})^2 - (\vec{p}_{\ell T} + \vec{p}_{\nu T})^2 . \quad (2.14)$$

When the missing energy comes only from the single neutrino from W decay, we expect to see a Jacobian peak $M_T(W) \sim M_W$, but this will not be so for the signal events where the missing energy is carried away by two massive particles in addition to the neutrino. This reconstructed variable is plotted in Fig. 6 for the signal and backgrounds. We see that a transverse mass cut, for example $M_T(W) > 220$ GeV, on the leptonic products can effectively

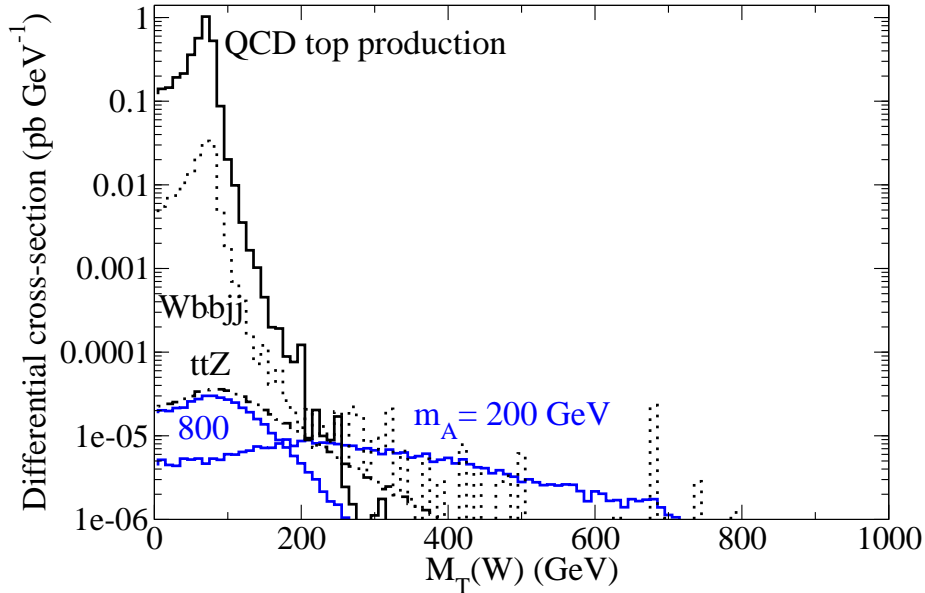


Figure 6: $M_T(W)$ distribution for both signal and background. The peak near M_W is prominent for the $t\bar{t}$ and $W(\rightarrow \ell\nu)bbjj$ backgrounds.

suppress the QCD $t\bar{t}$ and $Wbbjj$ backgrounds due to the presence of W production and its subsequent leptonic decay.

Note that we have not thus far taken advantage of the fact that the kinematics of SM $t\bar{t}$ in the semi-leptonic channel is fully reconstructible [28], following a well-known procedure in which the on-shell condition for the W boson is used to determine the four-momentum of the massless neutrino, upto a two-fold ambiguity. Imposing the on-shell condition for the leptonically-decaying top eliminates this ambiguity, while the mis-pairing for b and \bar{b} can be simultaneously reduced by minimizing the sum of the differences between the masses of the reconstructed tops and the actual top mass

$$(m_t - m(b_1jj))^2 + (m_t - m(b_2\ell\nu))^2. \quad (2.15)$$

Our detailed reconstruction procedure is summarized in Appendix B.

The situation is expected to be very different for the new physics signal in which the $t\bar{t}$ system recoils against the missing massive particles. Applying the same reconstruction technique to the signal events, one would therefore not expect to reconstruct the top quark successfully since the \cancel{E}_T contains a large contribution from the momenta of the A^0 s, which cannot be measured independently. This typically results in either not being able to find physical solutions for the longitudinal component of the missing energy, or in a reconstructed

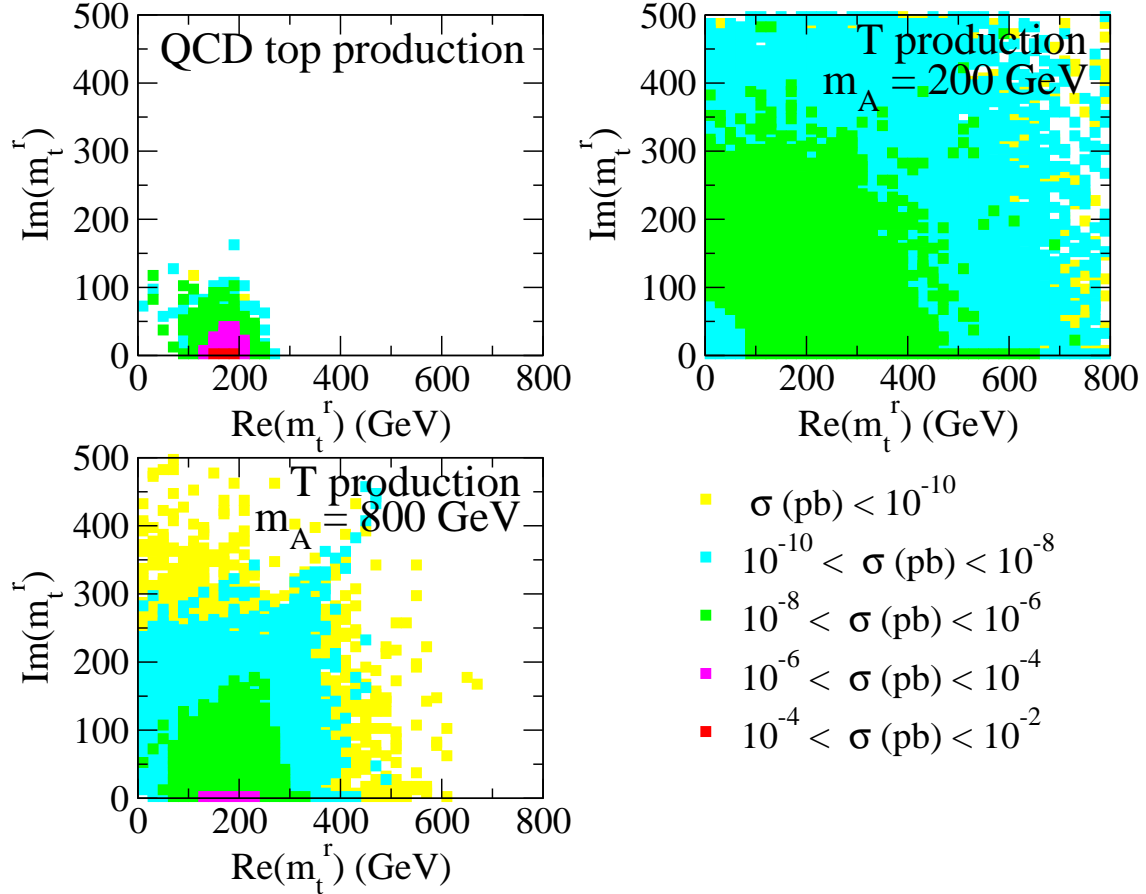


Figure 7: The reconstructed mass of the leptonically decaying top quark in the complex plane (a) for $t\bar{t}$ background, (b) for $m_A = 200$ GeV and (c) for $m_A = 800$ GeV. Allowing this variable to take on complex values serves as a pointer to new physics, an imaginary value is a signature of events with new missing particles.

mass that is very different from m_t . Therefore, this naive reconstruction procedure provides us with an effective way to distinguish the signal from the $t\bar{t}$ background. We encode the effect of unphysical momentum solutions by allowing the reconstructed top quark mass m_t^r to carry an imaginary part (see Appendix B for details). In this case, a large unphysical, *i.e.* imaginary, value for the reconstructed mass is a signature of events with missing particles beyond a single massless neutrino.

The results for the reconstructed $m_t^r = m(b_2\ell\cancel{E}_T)$ are shown in the complex plane in Fig. 7. As seen in Fig. 7(a), the reconstructed mass for the $t\bar{t}$ background is highly concentrated near m_t on the real axis although there are still a small number of events that give an unphysical top quark mass due to the energy-momentum smearing effects of the detectors. For the signal events, it is spread out over a large region as seen in Fig. 7(b) and (c). We are thus motivated

	$S : m_A = 200 \text{ GeV}$			$m_A = 800 \text{ GeV}$			$B : t\bar{t}$	$t\bar{t}Z$	$Wbbjj$
	eff.	S/B	S/\sqrt{B}	eff.	S/B	S/\sqrt{B}	eff.	eff.	eff.
Basic cuts	0.28	10^{-4}	0.2	0.32	10^{-4}	0.2	0.24	0.29	–
$\cancel{E}_T > 350$	0.65	0.1	4.3	$5 \cdot 10^{-4}$	$8 \cdot 10^{-5}$	$4 \cdot 10^{-3}$	$6 \cdot 10^{-4}$	0.03	$7 \cdot 10^{-3}$
$\cancel{E}_T > 600$	0.22	1.0	8.6	$9 \cdot 10^{-8}$	$4 \cdot 10^{-7}$	$4 \cdot 10^{-6}$	$2 \cdot 10^{-6}$	$2 \cdot 10^{-3}$	$8 \cdot 10^{-4}$
$ m_{jj} - M_W < 20$	0.97	10^{-4}	0.2	0.95	10^{-4}	0.2	0.96	0.89	0.11
$120 < m_t^{had} < 180$	0.76	10^{-4}	0.2	0.73	10^{-4}	0.2	0.77	0.72	0.10
$\phi_{t-b\ell} < 2.5$	0.75	$2 \cdot 10^{-4}$	0.3	0.54	$2 \cdot 10^{-4}$	0.2	0.26	0.50	0.31
$M_T(W) > 220$	0.62	0.7	13	0.03	$4 \cdot 10^{-2}$	0.7	$2 \cdot 10^{-5}$	0.11	$2 \cdot 10^{-3}$
$ m_t^r - 175 > 110$	0.75	$8 \cdot 10^{-3}$	1.5	0.08	$1 \cdot 10^{-3}$	0.2	$5 \cdot 10^{-5}$	0.17	0.30

Table 1: Effect of individual kinematical cuts on the signal for $m_T = 1 \text{ TeV}$ and backgrounds. All non-detector efficiencies are calculated for events which pass the basic cuts; masses and energies are in GeV. The statistical significance (S/\sqrt{B}) is computed for a luminosity of 100 fb^{-1} .

to impose a cut on $|m_t - m_t^r|$. The choice

$$|m_t - m_t^r| > 110 \text{ GeV} \quad (2.16)$$

for example, essentially eliminates the $t\bar{t}$ background. The range of unphysical values is reduced for the signal when the mass difference ΔM_{TA} becomes smaller, confirming the fact that when the missing A^0 s carry little kinetic energy, there is effectively no difference between the kinematics of the signal and $t\bar{t}$ background. In this kinematical regime the A^0 moves slowly and its momentum does not contribute significantly to \cancel{E}_T . Therefore we should be able to approximately reconstruct m_t by assuming $p_{\nu T} = \cancel{p}_T$.

To summarize the discussion in this section, we present in Table 1 the signal and background efficiencies after applying individual cuts, for all events that have passed the basic cuts. The table also includes the signal-to-background ratios S/B and statistical significance for signal observability S/\sqrt{B} for the individual cuts for an integrated luminosity of 100 fb^{-1} . From this we can see, for example, that for $m_T = 1 \text{ TeV}$, which has a production rate of about 0.045 pb at the LHC, a combination of an \cancel{E}_T cut and reconstructions of m_{jj} , $M_T(W)$ and the top mass can significantly reduce the background.

2.3 Discovery Reach

In this section we present the observational reach for our signal $T\bar{T} \rightarrow t\bar{t}A^0A^0 \rightarrow lbbjj + \cancel{E}_T$. We will choose our cuts based on the kinematical and reconstruction variables studied in the previous section. The particular choices we make here are designed to illustrate the potential of enhancing the signal-to-background ratio. A complete optimization of kinematical cuts can be based on our variable studies, but is not performed in this work.

Although the reconstruction of m_t^r is very effective in suppressing the $t\bar{t}$ background and distinguishing the signal, it does not provide a discrimination against the $Wbbjj$ background which does not have a real top quark to begin with. We thus impose additional cuts to reduce

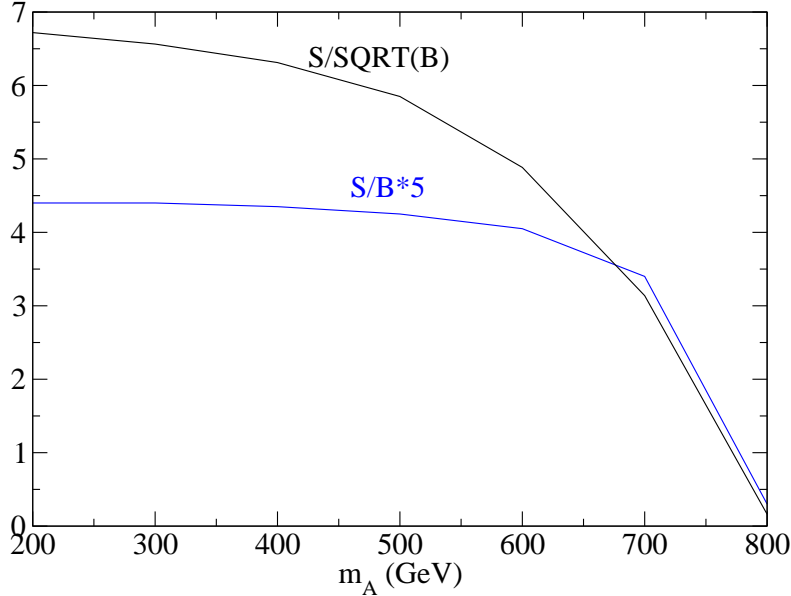


Figure 8: Signal-to-background ratio and the statistical significance (100 fb^{-1} integrated luminosity) as a function of m_A for a fermionic top partner of mass $m_T = 1 \text{ TeV}$.

this large background

$$70 \text{ GeV} < m_{jj} < 90 \text{ GeV}, \quad (2.17)$$

$$120 \text{ GeV} < m_t^r|_{\text{had}} = m(b_1 jj) < 180 \text{ GeV}, \quad (2.18)$$

where two b -tags are required for reconstruction.

The choice of an \cancel{E}_T cut is more involved. As discussed previously, on the one hand imposing an appropriate \cancel{E}_T cut will definitely help suppressing the background ($t\bar{t}Z$ in particular). On the other hand a large \cancel{E}_T cut will eliminate the signal for a small mass splitting. Hence we optimize the search by making a variable \cancel{E}_T cut

$$\cancel{E}_T > 0.2 \times \Delta M_{TA}. \quad (2.19)$$

We also impose the reconstructed leptonic top mass cut detailed in Eq. (2.16).

In Fig. 8, we present the signal-to-background ratio and statistical significance as a function of m_A for a fermionic top partner of mass $m_T = 1 \text{ TeV}$ and with 100 fb^{-1} integrated luminosity. We see that after imposing our proposed combination of cuts we have significant signal observability for a mass of upto $m_A \approx 750 \text{ GeV}$, which corresponds to $\Delta M_{TA} \sim 250 \text{ GeV}$. For an even smaller mass difference $\Delta M_{TA} \sim m_t$, it is still challenging to select out the signal.

We now study the more comprehensive reach in the two-parameter m_T - m_A plane with combined cuts. Our results are presented in Fig. 9 in the form of contour plots of signal

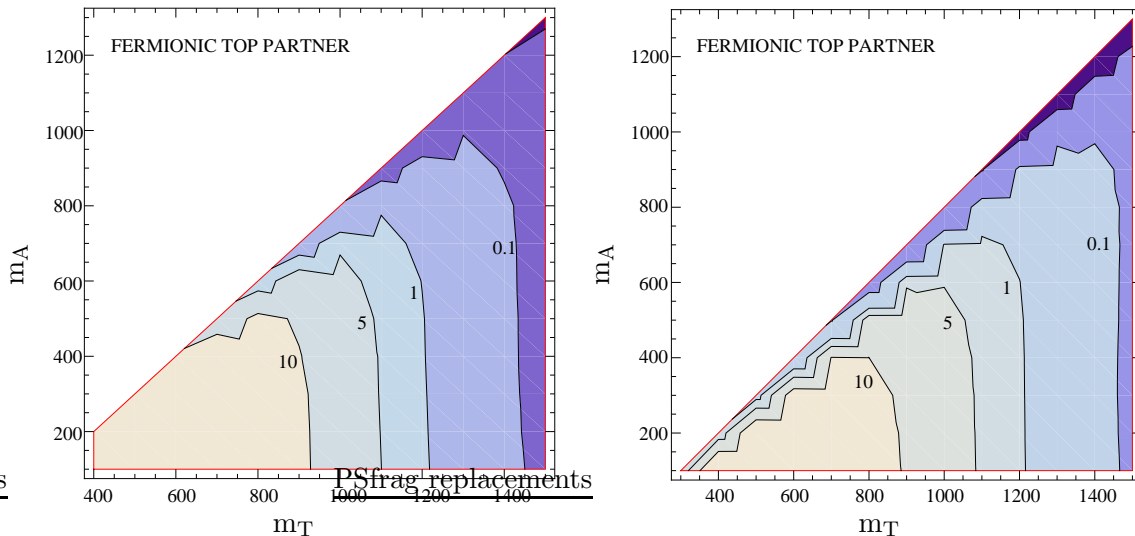


Figure 9: Contours of statistical significance for a fermionic top partner with 100 fb^{-1} of luminosity in the $m_T - m_A$ plane, the left-handed panel with the cuts described in this section; the right-hand panel with an additional cut on transverse mass $M_T(W) > 220 \text{ GeV}$.

observability for an integrated luminosity of 100 fb^{-1} , with 10σ , 5σ , and 1σ contours shown. In the left-hand panel we implement the cuts described in this section, while in the right-hand panel we include an additional cut on the W transverse mass $M_T(W) > 220 \text{ GeV}$. This additional cut does not enhance the signal significance (S/\sqrt{B}) appreciably due to correlations with other cuts, in particular $m_{\tilde{t}}^r$. It does however improve the signal to background ratio (S/B), and hence helps control systematic effects. We also note that the reach here is similar to that obtained in the fully hadronic mode [18]. It is straightforward to extend our results to the case of the scalar top partner decaying to tA^0 (e.g. $\tilde{t}_R \rightarrow t\chi_0$ in SUSY). As in the case of the fermionic top partner, the crucial parameter controlling much of the kinematics is the mass splitting $\Delta M_{TA} = m_{\tilde{t}} - m_{\chi_0}$. Given the same mass splitting, we expect the kinematics will be quite similar to the case of fermionic T .² Therefore, we should expect any difference in reach to be mostly due to the lower production cross section for the scalar top partner. The reach, with and without a transverse mass cut, is shown in Fig. 10.

3. Remarks on Distinguishing a Scalar Top Partner from a Fermion

As argued above, the hadron collider signatures of a fermionic top partner are expected to be very similar to those of scalar, making it challenging to directly measure the spin of the top partner at the LHC. We discuss several approaches to tackling this problem in this section.

²There are some subtle differences [18], which we will comment on in Sec. 3. We do not expect such differences to affect the discovery reach significantly.

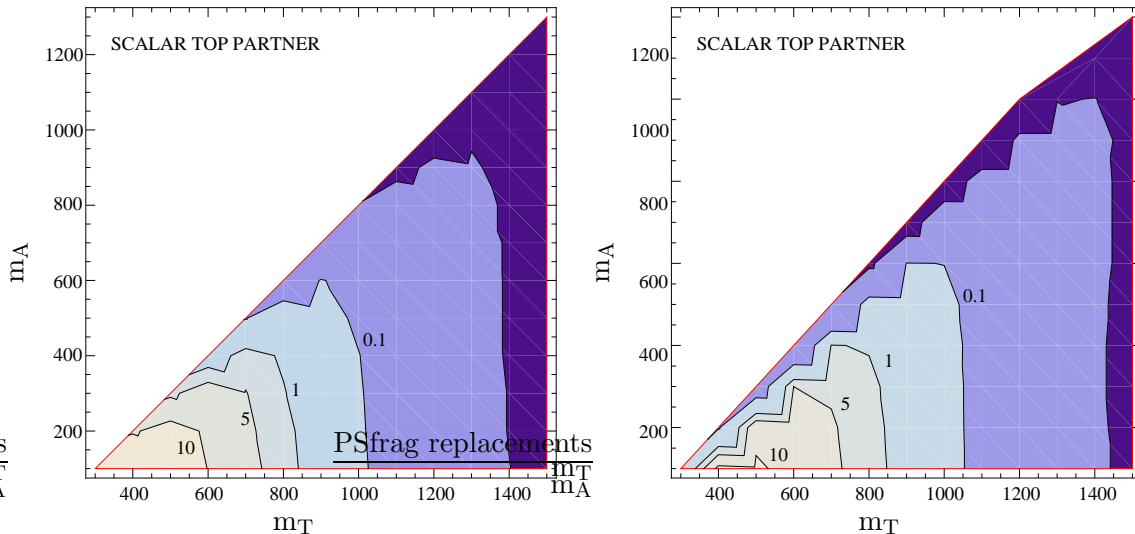


Figure 10: Contours of statistical significance for a scalar top partner, with 100 fb^{-1} of luminosity in the $m_T - m_A$ plane. The panel on the right is the result with an additional cut on transverse mass $M_T(W) > 220 \text{ GeV}$.

The most straightforward way to tell the fermionic partner from the scalar would be by using the difference in their production rates, as seen in Fig. 1. However, one cannot interpret this without making some assumption about the underlying model, since several degenerate scalars could be produced with the same total rate as a Dirac fermion of the same mass, for example. Even given some set of reasonable assumptions, as pointed out in Ref. [16, 18], we are left with the problem that masses cannot be measured directly (at least in the situation where there is more than one type of particle contributing to the missing energy) since most known observables only measure the mass difference. Consequently, a cross section measurement alone will not determine the particle’s mass or spin. Recently, several new methods have been proposed to tackle the problem of measuring absolute mass scale [29, 30]. However the reconstruction method in Ref. [29] relies on longer decay chains with more kinematical handles, and therefore is not directly applicable in our case. Application of the method in Ref. [30], which relies on accurately measuring the end point of the m_{T2} variable, to the case of minimal top partner decay has yet to be studied in this context.

Therefore, we have to rely on subtle kinematical differences. As a first example, based on the fact that a scalar would be lighter than a fermion with a given production cross section, we could try to look for some indication that the scalar is more boosted, using a parameter like the beamline asymmetry proposed in Ref. [18]

$$\text{BLA} = \frac{N_+^z - N_-^z}{N_+^z + N_-^z}, \quad (3.1)$$

where N_+^z (N_-^z) is the number of events with $p_{t_1}^z p_{t_2}^z > (<) 0$, for the momenta of the top quarks

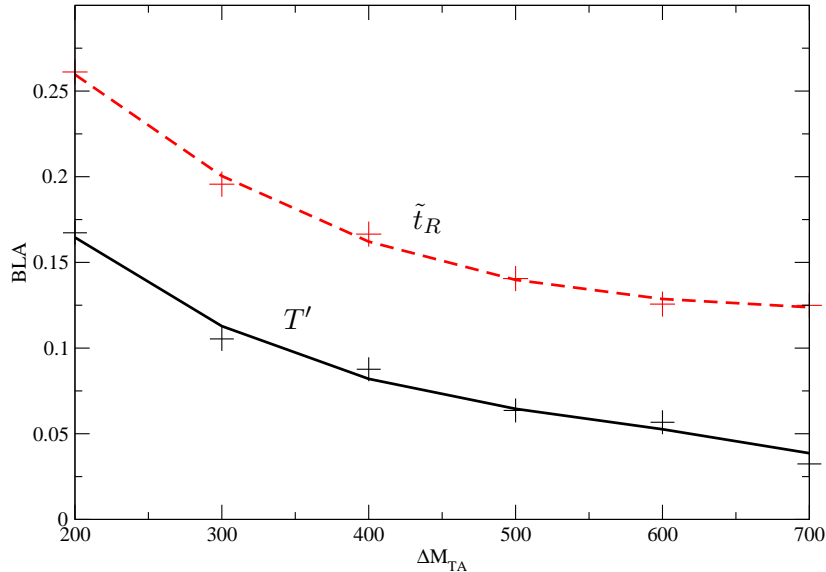


Figure 11: Beamline asymmetry (BLA) as a function of the mass difference between the top partner T and the lightest parity odd particle A_0 in a Little Higgs model (solid line) and SUSY (dashed line). Generator-level momenta are used for illustration, since events cannot be fully reconstructed.

p_{t_1} and p_{t_2} . The beam-line asymmetry for a \tilde{t}_R in SUSY and a T' in a Little Higgs model with the same production cross section is presented in Fig. 11. Note that we have not reconstructed the tops but simply used the known top momentum to illustrate the difference between the two cases. We remark that such a variable is also subject to several potential sources of error. First of all, the average boost will be sensitive to the parton distribution functions, which typically give rise to an error of 5–10%. More importantly, we must take into account the effect of the SM backgrounds [18]. Since the asymmetry for scalars and fermions are distinguishable at the 10% level, we typically need an accuracy of $S/\sqrt{S+B} \sim 10$ in order to have a statistically significant effect. From the results of Ref. [18], as well as this study, we see that such a high significance could be challenging for $m_T \sim 1$ TeV. Moreover, notice that the asymmetry decreases as the mass splitting increases, since for small mass splitting the top quarks produced are closer to the direction of T due to phase-space limitations. This will further limit the utility of such variables since, as we emphasized in this study, we will certainly have more statistics for the signal with larger mass splittings. We also note that constructing an analog of this observable in the semi-leptonic channel, where some information about the top momentum will be inevitably lost, is less straightforward. One may need to rely on the partially reconstructed top momentum $p_b + p_\ell$ in the leptonic decay. As a result, we expect

the mass information contained in the beamline asymmetry variable to be less prominent.

Using information about the production angular distributions to distinguish between fermionic and bosonic top partners will be challenging as well due to the presence of the additional missing neutrino, which makes the top quark reconstruction more difficult. Obtaining clues from the directions of the visible decay products is possible, but since these are also significantly affected by other factors such as the boost of the top partner, the phase space, and the chirality of its coupling to the top quark, we expect any information about the original production matrix element to be washed out. Even if we are able to obtain such information, relating it to the spin of the top partner is not at all straightforward. Unlike processes such as $Z \rightarrow \ell^+ \ell^-$, pair production of top partners is not dominated by a single s-channel process. Therefore, several partial waves may contribute, making a distinction between fermion and boson potentially challenging.

We now comment on spin-determination strategies using invariant mass distributions of objects in long decay chains [31]. Consider a decay chain $X \rightarrow a + Y^{(*)} (\rightarrow b + Z)$, where a, b are observable SM particles and X, Y and Z are new particles beyond the SM, with Y either on or off-shell. In this case, the invariant mass distribution m_{ab} carries information about the spin of the *intermediate* particle Y . In particular, it is a polynomial of order $2J_Y$. Such a strategy will not be applicable in the simple decay $T \rightarrow t + A^0$ of our current interest, since T is in the initial state. If instead of this minimal setup, there is an extended top-partner sector, with the possibility of it decaying through a longer decay chain, we could in principle extract more information. For example, if the top partner decays via $T \rightarrow b + W_H (\rightarrow W + A^0)$, the spin of W -partner W_H could in principle be measured by studying the correlation between b and W . Then, assuming Lorentz invariant and renormalizable interactions, we could infer the spin of the top partner. Considering this to be a plausible scenario, it seems worthwhile carrying out a more detailed study and quantifying the observational feasibility for this channel.

4. Summary and Conclusions

We have studied methods of extracting the new physics signal in the $t\bar{t} + \cancel{E}_T$ final state, with the tops decaying semi-leptonically. We have developed kinematical variables that optimally separate the signal from the SM backgrounds. The leading background is $t\bar{t}$ production from QCD. The other two large backgrounds are $Wb\bar{b}jj$ and $t\bar{t}Z$. We found the following kinematical variables useful:

- A cut on missing transverse energy can effectively remove the $t\bar{t}Z$;
- Looking inside the mass windows $m_{jj} \approx M_W$ and $m_{bjj} \approx m_t$ for the hadronically-decaying top will suppress $Wb\bar{b}jj$;
- The back-to-back nature of $t\bar{t}$ (or realistically $\phi_{t-b\ell}$) can be used to select against backgrounds;

- The reconstruction of the transverse mass $M_T(W)$ can effectively single out background events with a neutrino as the only missing particle;
- Extending the definition of the reconstructed top mass m_t^r in the leptonic mode to include unphysical values can effectively separate out the large $t\bar{t}$ background.

In all the cases, if the mass difference is small $\Delta M_{TA} \sim 200 - 300$ GeV, then the signal kinematics, which are very much like those for $t\bar{t}$ production, are very difficult to observe above the backgrounds. The signal observability is summarized in Figs. 9 and 10.

We have also commented on possible ways to distinguish between two typical examples of such new physics: a \tilde{t}_R in SUSY from a T' in models with a fermionic top partner. Such methods include using the difference in the production rate, measuring angular correlations, and possibly exploring differences in the T' and \tilde{t}_R couplings. We concluded that none of these methods provide an easy determination of the spin of the top partner in this particular channel, with only the minimal decay pattern assumed in this study we are likely to have to explore more subtle kinematical distributions, either to obtain a handle on the absolute mass scale or precisely measure the production and decay matrix elements, or both at the same time. We also note that if the new physics including the top partner is beyond the minimal framework that we have focused on, this generically makes both the detection and measurement of the properties of the top partner easier. It would be interesting to explore some of these possibilities in some detail.

5. Acknowledgement

We are grateful for discussions with Nima Arkani-Hamed, Robin Erbacher, Henry Frisch, Kyoungchul Kong, Partick Meade and Mihoko Nojiri. We would also like to thank the Aspen Center for Physics where part of the work was completed, for its hospitality. The work of T.H. was supported in part by the US DOE under contract No. DE-FG02-95ER40896 and in part by the Wisconsin Alumni Research Foundation. The work of L.W. is supported by the National Science Foundation under Grant No. 0243680 and the Department of Energy under grant No. DE-FG02-90ER40542. Fermilab is operated by Fermi Research Alliance, LLC under Contract No. DE-AC02-07CH11359 with the United States Department of Energy. The part of this research carried out at KITP was supported by the National Science Foundation under Grant No. PHY05-51164. Any opinions, findings, and conclusions or recommendations expressed in this material are those of the authors and do not necessarily reflect the views of the National Science Foundation.

A. Definitions of Transverse Variables

In general, a transverse mass variable can be formally defined by projecting the momenta to the plane perpendicular to the beam direction

$$M_T^2 = \left(\sum_i E_{iT} \right)^2 - \left(\sum_i \vec{p}_{iT} \right)^2, \quad (\text{A.1})$$

$$E_{iT} = \sqrt{m_i^2 + \vec{p}_{iT}^2}, \quad (\text{A.2})$$

where $E_T = |\vec{p}_T|$ for a massless particle.³ If there are unobservable particles, such as neutrinos or new stable neutral particles, then the missing transverse energy (or momentum) is defined by

$$\vec{E}_T = \vec{p}_T = - \sum_o \vec{p}_{oT}. \quad (\text{A.3})$$

where \vec{p}_{oT} are the transverse momenta of the visible particles in the event. Two remarks are in order here. First, the mass information for a missing particle is lost in the above definition. Second, if we consider the complete system of an event as in Eq. (A.1), then the second term vanishes as a consequence of Eq. (A.3). This leads to a simple relation

$$M_T = \sum_i E_{iT}. \quad (\text{A.4})$$

In its simplest form, one can just sum over the transverse momentum of each individual observable (massless) particles to obtain the so-called “effective transverse mass”,

$$M_T^{\text{eff}} = \sum_o E_{oT} + E_T \quad (\text{A.5})$$

Alternatively, one may consider the “cluster transverse mass”

$$M_T^c = \sqrt{m_c^2 + \vec{p}_{cT}^2} + E_T, \quad (\text{A.6})$$

where $m_c^2 = (\sum_o p_o)^2$ and $\vec{p}_{cT} = -\vec{E}_T$.

B. Top Reconstruction in Semileptonic Mode

First consider the QCD $t\bar{t}$ production, with one top quark decaying hadronically and the other leptonically. Identifying the observed missing transverse momentum to be from a missing neutrino, the conservation of transverse momentum gives

$$p_{\nu T} = - \sum_{\text{visible}} p_T = \not{p}_T \quad (\text{B.1})$$

We also use mass-shell conditions for the neutrino and the leptonically-decaying W .

$$p_\nu^2 = 0 \quad (\text{B.2})$$

$$(p_\nu + p_l)^2 = 2p_\nu \cdot p_l = M_W^2 \quad (\text{B.3})$$

We can then solve for $p_{\nu L}$ to obtain, subject to the two-fold ambiguity,

$$p_{\nu L} = \frac{p_{lL}(M_W^2 - 2\not{p}_T \cdot p_{lT}) \pm \sqrt{\Delta}}{2(E_l^2 - p_{lL}^2)} \quad (\text{B.4})$$

³Experimentally, the transverse energy is the quantity measured by the calorimeters; while the transverse momentum is determined by the charge tracking system.

where Δ is defined as

$$\Delta = E_l^2 [M_W^4 - 4M_W^2 \not{p}_T \cdot p_{l_T} + 4(p_{l_T} \cdot \not{p}_T)^2 - 4(E_l^2 - p_{l_L}^2) \not{p}_T^2] \quad (\text{B.5})$$

The correct solution for p_ν can be picked by enforcing that the leptons plus b reconstruct the top quark. Grouping the wrong b -quark with the leptons can be avoided by enforcing that the hadronic jets also reconstruct the top quark. In other words our solution should minimize the following quantity, where m_i stands for the invariant mass of the reconstructed top quark on the i th fermionic leg:

$$\sum_{i=l, h} |m_i^2 - m_t^2| \quad (\text{B.6})$$

If we apply the same reconstruction procedure to the top quarks in $T\bar{T}$ production, since we are overlooking the fact that some of the missing energy in the event comes from the A^0 s, rather than the neutrino, there is no reason why our solution should correspond to anything physical. In fact, in general Δ might even be a negative quantity, and we need a prescription to deal with this case.

We thus propose to generalize p_ν and m_t^2 to be complex quantities. When $\Delta < 0$, we define

$$p_{\nu_L} = R_{\nu_L} \pm iI_{\nu_L}, \quad (\text{B.7})$$

$$E_\nu = R_{\nu_E} \pm iI_{\nu_E} = R_{\nu_E} \pm iI_{\nu_L} \frac{p_{l_L}}{E_l}, \quad (\text{B.8})$$

where R , I 's are given in terms of the known quantities p_l, \not{p}_T, M_W as before. For definitiveness, we keep the $+$ sign for the solutions. We then reconstruct the complex top-quark mass

$$(m_t^r)^2 = (p_l + p_\nu + p_b)^2 = (E_l + E_b + R_{\nu_E} + iI_{\nu_E})^2 \quad (\text{B.9})$$

$$- (p_{lT} + p_{bT} + \not{p}_T)^2 - (p_{lL} + p_{bL} + R_{\nu_L} + iI_{\nu_L})^2. \quad (\text{B.10})$$

The size of the imaginary part is a good measure of how ‘‘far away’’ from SM $t\bar{t}$ production the event is.

References

- [1] S. Dimopoulos and H. Georgi, Nucl. Phys. B **193**, 150 (1981).
- [2] A. G. Cohen, D. B. Kaplan and A. E. Nelson, Phys. Lett. B **388**, 588 (1996) [arXiv:hep-ph/9607394].
- [3] For a recent Working Group Report on non-standard Higgs physics, see *e.g.*, S. Kraml *et al.*, arXiv:hep-ph/0608079.
- [4] S. Weinberg, Phys. Rev. D **13**, 974 (1976); L. Susskind, Phys. Rev. D **20**, 2619 (1979).

- [5] C. T. Hill, Phys. Rev. D **24**, 691 (1981); C. T. Hill, Phys. Lett. B **266**, 419 (1991); R. S. Chivukula, B. A. Dobrescu, H. Georgi and C. T. Hill, Phys. Rev. D **59**, 075003 (1999) [arXiv:hep-ph/9809470].
- [6] B. A. Dobrescu and C. T. Hill, Phys. Rev. Lett. **81**, 2634 (1998) [arXiv:hep-ph/9712319].
- [7] For a survey of strong dynamics for electroweak physics see C. T. Hill and E. H. Simmons, Phys. Rept. **381**, 235 (2003) [Erratum-ibid. **390**, 553 (2004)] [arXiv:hep-ph/0203079] and the references therein.
- [8] T. Gherghetta and A. Pomarol, Nucl. Phys. B **586**, 141 (2000) [arXiv:hep-ph/0003129]. K. Agashe, A. Delgado, M. J. May and R. Sundrum, JHEP **0308**, 050 (2003) [arXiv:hep-ph/0308036].
- [9] D. B. Kaplan, H. Georgi and S. Dimopoulos, Phys. Lett. B **136**, 187 (1984).
- [10] N. Arkani-Hamed, A. G. Cohen and H. Georgi, Phys. Lett. B **513**, 232 (2001) [arXiv:hep-ph/0105239]; For a review on Little Higgs models see M. Schmaltz and D. Tucker-Smith, Ann. Rev. Nucl. Part. Sci. **55**, 229 (2005) [arXiv:hep-ph/0502182].
- [11] N. Arkani-Hamed, S. Dimopoulos and G. R. Dvali, Phys. Lett. B **429**, 263 (1998) [arXiv:hep-ph/9803315].
- [12] L. Randall and R. Sundrum, Phys. Rev. Lett. **83**, 3370 (1999) [arXiv:hep-ph/9905221].
- [13] T. Appelquist, H. C. Cheng and B. A. Dobrescu, Phys. Rev. D **64**, 035002 (2001) [arXiv:hep-ph/0012100].
- [14] Z. Chacko, H. S. Goh and R. Harnik, Phys. Rev. Lett. **96**, 231802 (2006) [arXiv:hep-ph/0506256].
- [15] H. C. Cheng and I. Low, JHEP **0309**, 051 (2003) [arXiv:hep-ph/0308199]. H. C. Cheng and I. Low, JHEP **0408**, 061 (2004) [arXiv:hep-ph/0405243]. I. Low, JHEP **0410**, 067 (2004) [arXiv:hep-ph/0409025].
- [16] H. C. Cheng, I. Low and L. T. Wang, Phys. Rev. D **74**, 055001 (2006) [arXiv:hep-ph/0510225].
- [17] K. Agashe, A. Belyaev, T. Krupovnickas, G. Perez and J. Virzi, Phys. Rev. D **77**, 015003 (2008) [arXiv:hep-ph/0612015]. V. Barger, T. Han and D. G. E. Walker, Phys. Rev. Lett. **100**, 031801 (2008) [arXiv:hep-ph/0612016]. B. Lillie, L. Randall and L. T. Wang, JHEP **0709**, 074 (2007) [arXiv:hep-ph/0701166]. A. L. Fitzpatrick, J. Kaplan, L. Randall and L. T. Wang, JHEP **0709**, 013 (2007) [arXiv:hep-ph/0701150]. K. Agashe, H. Davoudiasl, G. Perez and A. Soni, Phys. Rev. D **76**, 036006 (2007) [arXiv:hep-ph/0701186]. U. Baur and L. H. Orr, Phys. Rev. D **76**, 094012 (2007) [arXiv:0707.2066 [hep-ph]]. R. Frederix and F. Maltoni, arXiv:0712.2355 [hep-ph]. U. Baur and L. H. Orr, arXiv:0803.1160 [hep-ph].
- [18] P. Meade and M. Reece, Phys. Rev. D **74**, 015010 (2006) [arXiv:hep-ph/0601124].
- [19] A. Freitas and D. Wyler, JHEP **0611**, 061 (2006) [arXiv:hep-ph/0609103]. A. Belyaev, C. R. Chen, K. Tobe and C. P. Yuan, arXiv:hep-ph/0609179.
- [20] S. Matsumoto, M. M. Nojiri and D. Nomura, Phys. Rev. D **75**, 055006 (2007) [arXiv:hep-ph/0612249]; M. M. Nojiri and M. Takeuchi, arXiv:0802.4142 [hep-ph].
- [21] H. L. Lai *et al.*, Phys. Rev. D **55**, 1280 (1997) [arXiv:hep-ph/9606399].

- [22] T. Sjostrand, S. Mrenna and P. Skands, *JHEP* **0605**, 026 (2006) [arXiv:hep-ph/0603175].
- [23] M. L. Mangano, M. Moretti, F. Piccinini, R. Pittau and A. D. Polosa, *JHEP* **0307**, 001 (2003) [arXiv:hep-ph/0206293].
- [24] “ATLAS detector and physics performance. Technical design report. Vol. 2”, CERN-LHCC-99-15.
- [25] “CMS Physics: Technical Design Report V.2: Physics Performance”, CERN-LHCC-2006-021.
- [26] V. D. Barger, A. D. Martin and R. J. N. Phillips, *Phys. Lett. B* **125**, 339 (1983).
- [27] C. G. Lester and D. J. Summers, *Phys. Lett. B* **463**, 99 (1999) [arXiv:hep-ph/9906349]. A. Barr, C. Lester and P. Stephens, *J. Phys. G* **29**, 2343 (2003) [arXiv:hep-ph/0304226].
- [28] B. Abbott *et al.* [D0 Collaboration], *Phys. Rev. D* **58**, 052001 (1998) [arXiv:hep-ex/9801025]. F. Abe *et al.* [CDF Collaboration], *Phys. Rev. Lett.* **80**, 2767 (1998) [arXiv:hep-ex/9801014].
- [29] H. C. Cheng, J. F. Gunion, Z. Han, G. Marandella and B. McElrath, arXiv:0707.0030 [hep-ph]. H. C. Cheng, D. Engelhardt, J. F. Gunion, Z. Han and B. McElrath, arXiv:0802.4290 [hep-ph].
- [30] W. S. Cho, K. Choi, Y. G. Kim and C. B. Park, arXiv:0709.0288 [hep-ph]. B. Gripaios, arXiv:0709.2740 [hep-ph]. A. J. Barr, B. Gripaios and C. G. Lester, *JHEP* **0802**, 014 (2008) [arXiv:0711.4008 [hep-ph]]. W. S. Cho, K. Choi, Y. G. Kim and C. B. Park, *JHEP* **0802**, 035 (2008) [arXiv:0711.4526 [hep-ph]]. G. G. Ross and M. Serna, arXiv:0712.0943 [hep-ph]. M. M. Nojiri, G. Polesello and D. R. Tovey, arXiv:0712.2718 [hep-ph].
- [31] A. J. Barr, *Phys. Lett. B* **596**, 205 (2004) [arXiv:hep-ph/0405052]. J. M. Smillie and B. R. Webber, *JHEP* **0510**, 069 (2005) [arXiv:hep-ph/0507170]. A. Alves, O. Eboli and T. Plehn, *Phys. Rev. D* **74**, 095010 (2006) [arXiv:hep-ph/0605067]. A. J. Barr, *JHEP* **0602**, 042 (2006) [arXiv:hep-ph/0511115]. L. T. Wang and I. Yavin, *JHEP* **0704**, 032 (2007) [arXiv:hep-ph/0605296]. J. M. Smillie, *Eur. Phys. J. C* **51**, 933 (2007) [arXiv:hep-ph/0609296]. C. Kilic, L. T. Wang and I. Yavin, *JHEP* **0705**, 052 (2007) [arXiv:hep-ph/0703085]. C. Csaki, J. Heinonen and M. Perelstein, arXiv:0707.0014 [hep-ph].
For a recent review, see L. T. Wang and I. Yavin, arXiv:0802.2726 [hep-ph].